Journal of Non-Crystalline Solids 576 (2022) 121242

Contents lists available at ScienceDirect

Journal of Non-Crystalline Solids

journal homepage: www.elsevier.com/locate/jnoncrysol

Rare earth added barium alumino borosilicate glass-ceramics as sealants in solid oxide fuel cells

M.S. Salinigopal [a,b], N. Gopakumar [b], P.S. Anjana [a,*], O.P. Pandey [c]

[a] Department of Physics, All Saints' College, University of Kerala, Trivandrum, Kerala, India 695007
[b] Post Graduate Department of Physics, Mahatma Gandhi College, Research Centre, University of Kerala, Trivandrum, Kerala, India 695004
[c] School of Physics and Materials Science, Thapar Institute of Engineering & Technology, Patiala, Punjab 147004, India

ARTICLE INFO

Keywords:
Glass-ceramics
X-ray diffraction (XRD)
Density
Co-efficient of thermal expansion (CTE)
Interconnect

ABSTRACT

Glasses with composition 50BaO-(5-x) Al_2O_3-xR_2O_3–30B_2O_3–15SiO_2 (x = 0,5 and R = Nd, Gd, La, Dy) have been synthesized by conventional melt quenching method. Controlled crystallization has been carried out to convert these glasses to corresponding glass-ceramics. X-ray diffraction (XRD) technique has been used to identify the crystalline phases formed in glass-ceramics. Archimede's method has been used to measure the density of glass-ceramics. The co-efficient of thermal expansion of all glass-ceramics lie within the range (11.60 – 12.81) x 10^{-6}/°C, which matches with that of the other components of solid oxide fuel cell. The interaction study of glass-ceramics with Crofer22APU interface and Crofer22APU/Glass-ceramic/Crofer22APU showed no evidence of interfacial failure and cracks. Hence the prepared glass-ceramics can be considered as a suitable candidate for sealant materials in SOFC applications.

1. Introduction

Solid oxide fuel cell (SOFCs) is an emerging energy technology which has many advantages over existing technologies; high electrical conversion efficiency (over 60%), potential for carbon capture, no NO_2 emission, fuel flexibility, low noise, and suppleness for transportation and stationary applications. This technology may be a panacea for carbon capture visible of the separate fuel and air flow systems [1–3]. SOFC has lower manufacturing cost and better power density as compared to other fuel cells, but it requires gas tight hermetic sealants. Due to the high operating temperature (600–1000 °C), selection of components may be a crucial challenge for SOFC applications. The operating temperature of SOFC is restricted by electrochemical reaction that affects the efficiency of cell performance. High operating temperature is a bonus for fuel utilization and for performance of a SOFC system. However the cost of the materials and also the lack of long term stability are the most disadvantages of this technology. Hence the recent research focuses on the event of intermediate SOFC with an operating temperature range of 600 °C–800 °C. This can reduce the system cost and more over enhance the long-term stability [3].

One of the most important challenges for intermediate temperature SOFC technology is that the development of suitable sealing materials to separate fuel and air. Reliable seals must be capable of tolerating high temperature operations above 500 °C and rigorous oxidizing and reducing environments. The seals also have to maintain long-term performance stability at the operating temperature and endure thermal cycles during routine operation. For obtaining a hermetic seal/interconnect interface, some basic requirements must be fulfilled. Firstly, glass-ceramic seal should bond strongly in addition as adhere well to the interconnect. Secondly, the interface should be very thin in order that the residual stresses at the interface are minimum. In addition to this, at seal-interconnect interface, diffusion of chromium from interconnect (interconnects having Cr content like Crofer22APU) into glass seal should be minimal. Diffusion of glass seal constituents into the interconnect should even be avoided so as to retain stable network structure [4].

Glass and glass-ceramic sealants are developed due to their extremely low leakage rate at SOFC operation temperature. The thermal properties and viscosity of glass based sealants is tailored by tuning the composition and crystalline volume fraction of the glass matrix to satisfy the wants for sealing materials [5,6]. Seals must have long-term stability and not cause degradation of adjacent materials at the elevated temperatures and within the harsh environments typical to SOFC operation. The performance and life time of a seal reply upon the degree to which

* Corresponding author at: Department of Physics, All Saints' College, Thiruvananthapuram, Kerala, India 695007.
E-mail addresses: psanjanaa@yahoo.com, psanjana@gmail.com (P.S. Anjana).

https://doi.org/10.1016/j.jnoncrysol.2021.121242
Received 5 August 2021; Received in revised form 17 October 2021; Accepted 18 October 2021
Available online 11 November 2021
0022-3093/

Table 1
The composition of glass-ceramics for interaction study.

Sample code	Composition (mol%)							
	BaO	Al_2O_3	Nd_2O_3	Gd_2O_3	Dy_2O_3	La_2O_3	B_2O_3	SiO_2
BABS	50	5	–	–	–	–	30	15
BNBS-5	50	0	5	–	–	–	30	15
BGBS-5	50	0	–	5	–	–	30	15
BDBS-5	50	0	–	–	5	–	30	15
BLBS-5	50	0	–	–	–	5	30	15

gas flows within the fabric and at the interface is inhibited. Therefore, failure of seals is that the results of cracking/damage within the bulk and gaps or separation at the interface [7].

Glass–ceramics are extensively studied due to the wide range of properties available by way of the modification of composition. Alkaline earth metal based silicate glasses and glass-ceramics are reported to be potential materials as sealants for such applications [8]. Alkaline earth-based aluminosilicate glasses had been extensively studied as candidate for sealing glasses. Sohn et al. had investigated the thermal and chemical stability of the $BaO–Al_2O_3–La_2O_3–SiO_2–B_2O_3$system. They found that the CTE increased with BaO content and a maximum value of $\sim 11 \times 10^{-6}\ ^{\circ}C^{-1}$ is obtained for 40% of BaO and $B_2O_3/SiO_2 = 0.7$ [9]. Ley et al. studied the $SrO–Al_2O_3–La_2O_3–SiO_2–B_2O_3$ glass system with varying CTE within the range of (8–13) $\times\ 10^{-6}\ ^{\circ}C^{-1}$ [10]. Amongst different glass systems, the SiO_2 rich alkaline earth metal system has been identified collectively of the foremost promising one for SOFC application [11].

The present study reports the interaction between Crofer22APU interconnect and 50BaO-(5-x)Al_2O_3-xR_2O_3–30B_2O_3–15SiO_2($x = 0,5$ and R = Nd, Gd, Dy, La) glass-ceramics by varying the rare earth ions.

2. Materials and methods

Barium alumino borosilicate glasses with composition 50BaO-(5-x)

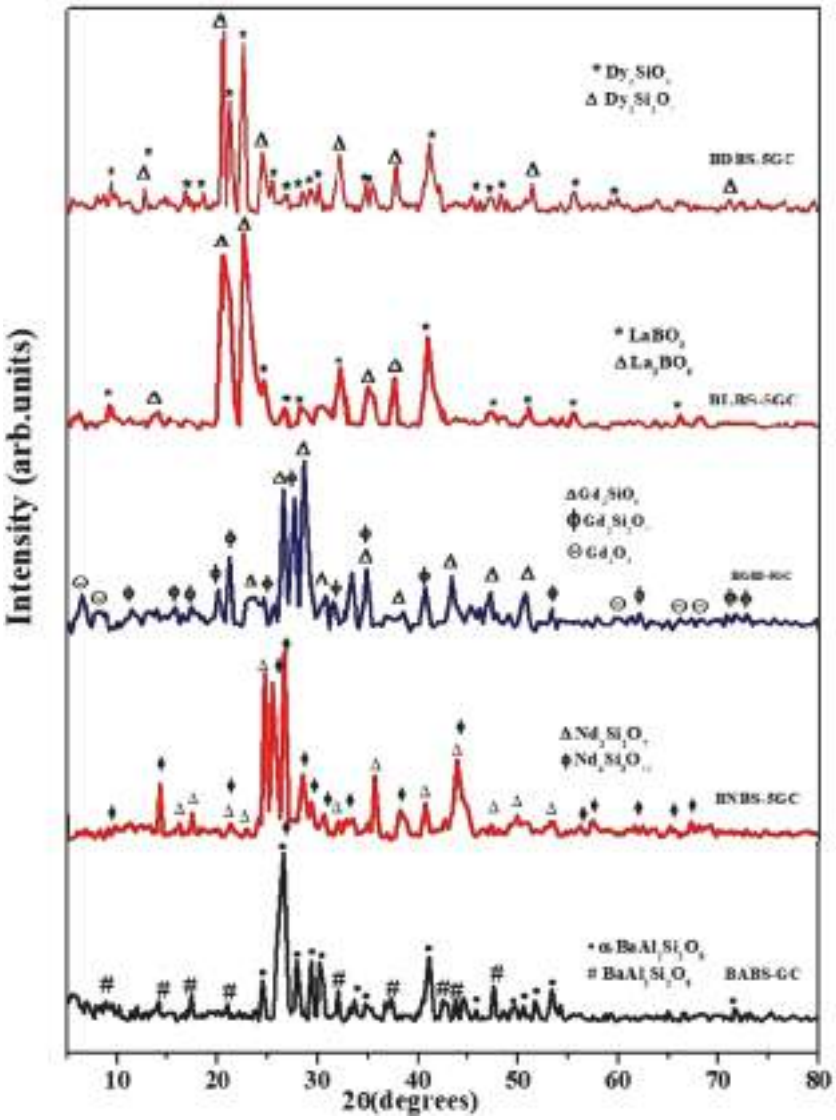

Fig. 1. XRD patterns of 50BaO-(5-x) Al_2O_3- xR_2O_3–30B_2O_3–15SiO_2 (x = 0, 5 and R = Nd, Gd, La, Dy) glass-ceramics.

Al_2O_3-xR_2O_3–30B_2O_3–15SiO_2 (x = 0, 5 and R = Nd, Gd, Dy, La) were prepared by normal melt quench method. The oxides/carbonates [$BaCO_3$ (99.9%), B_2O_3 (99.9%), SiO_2 (99.9%), Al_2O_3 (99.9%), Nd_2O_3(99.9%), Gd_2O_3(99.9%), La_2O_3(99.9%) and Dy_2O_3 (99.9%)] purchased from Sigma Aldrich were used as raw materials. The stoichiometric amounts of these chemicals were mixed in an agate mortar for 2 h with distilled water as medium. The powders were dried in an electric oven and melted in a platinum crucible. Depending on the composition, glasses were melted in the temperature range 1250 to 1285 °C. The melts were poured into a pre-heated brass mould and then immediately transferred into a preheated muffle furnace for annealing at 350 °C for 2 h to remove the residual stress due to temperature gradient, which is produced by rapid cooling. After annealing the glass samples were cooled to room temperature. Finally, the transparent glasses were formed. Depending on the composition of the glasses, they were heat treated in the range 800–920 °C to form glass-ceramics (Table 1).

The structural analysis was done using X-ray diffractometer (Bruker AXS D8 Advance, Germany) with CuK_α radiation having a wavelength of 1.5406 Å to identify the formation of crystalline phases in glass-ceramics. The densities of the glass-ceramics were measured by Archimedes principle using water as immersion liquid. The co-efficient of thermal expansion of glasses and glass-ceramic samples were measured with a push rod dilatometer (DIL 402 PC Netzsch, Germany) at a heating rate of 10 °C/min and within the temperature range 30–600 °C. Flat surfaces of the cylindrical pellets of thickness 6 - 7 mm were used for the CTE measurements. In order to find out the suitability of the presently prepared glass-ceramics as sealing materials in SOFC, an interaction study of glass-ceramic with interconnect material was done. In the present study, we used Crofer22APU as interconnect material. Fine powder of glass-ceramics was mixed with 5% PVA in ethanol and this paste was used as filling material between two plates of Crofer22APU with dimension 1 × 1 cm^2. This diffusion couple was heat treated at 700 °C for 10 h in oxidizing atmosphere. After taking the cross-section of the heat-treated samples, they were mounted in epoxy, ground and polished to a mirror like finish. The polished samples were lightly etched with HF and coated by gold. The microstructure was observed using Scanning Electron Microscope (EVO-ZEISS).

3. Results and discussions

3.1. X-ray diffraction studies (XRD)

X-ray diffraction (XRD) patterns of glass–ceramics are given in Fig. 1. Crystalline peaks are observed in glass-ceramics. The patterns observed from the heat treated samples show a reduction in the amorphous hump and the development of peaks corresponding to the formation of new crystalline phases that are identified using ICDD database files. The crystalline phases present in the 50BaO-5Al_2O_3–30B_2O_3–15SiO_2 glass-ceramic are $BaAl_2Si_2O_8$, α-$BaAl_2Si_2O_8$ and $BaSiO_3$ and are confirmed by comparing the standard data with ICDD card numbers 88–1048 for α-$BaAl_2Si_2O_8$ (Hexagonal), 38–1450 for $BaAl_2Si_2O_8$ (Monoclinic) and 70–2112 for $BaSiO_3$ (orthorhombic).

In the case of Nd_2O_3, Gd_2O_3 and Dy_2O_3 added systems, the less stable monoclinic celsian ($BaAl_2Si_2O_8$) phase is replaced by more stable silicate based crystalline phases such as $Nd_2Si_2O_7$ (tetragonal) and $Nd_4Si_3O_{12}$ (hexagonal) for Nd_2O_3 added systems, Gd_2SiO_5 (monoclinic), $Gd_2Si_2O_7$ (orthorhombic) for Gd_2O_3 added systems and $Dy_2Si_2O_7$ and Dy_2SiO_5 for Dy_2O_3 added systems. The formation of these phases is confirmed by comparing with ICDD card numbers 89–5347, 42–0171, 74–1795, 72–2062, 46–0398 and 40–0289 for $Nd_2Si_2O_7$, $Nd_4Si_3O_{12}$, Gd_2SiO_5, $Gd_2Si_2O_7$ and $Dy_2Si_2O_7$ and Dy_2SiO_5 phases respectively. In the case of La_2O_3 added systems, the monoclinic celsian ($BaAl_2Si_2O_8$) phase is replaced by the borate based crystalline phases such as La_3BO_6 and $LaBO_3$. The formation of these phases is confirmed by comparing with ICDD card numbers 50–1379, 73–1149 respectively. Celsian exist in two polymorphs such as hexacelsian (α-$BaAl_2Si_2O_8$) and monocelsian ($BaAl_2Si_2O_8$) [12]. Bahadur et al., had reported that during initial stages of crystallization, Si rich phases are nucleated in the glass matrix and in the later stage, other cations occurred the site during crystallization [13]. In the present study, less symmetric phases such as hexacelsian (α-$BaAl_2Si_2O_8$) and celsian ($BaAl_2Si_2O_8$) are formed in 50BaO-5A-l_2O_3-xR_2O_3–30B_2O_3–15SiO_2 glass-ceramics. With the addition of rare earth oxides, the amount of hexacelsian (α-$BaAl_2Si_2O_8$) and celsian ($BaAl_2Si_2O_8$) phases decreased and rare earth oxides. based crystalline phases are formed which leads to the creation of more stable glass-ceramics The formation of crystalline phase depends on the chemical nature of the intermediate oxides and the existing local arrangement of the cations within the glass matrix [13,14].

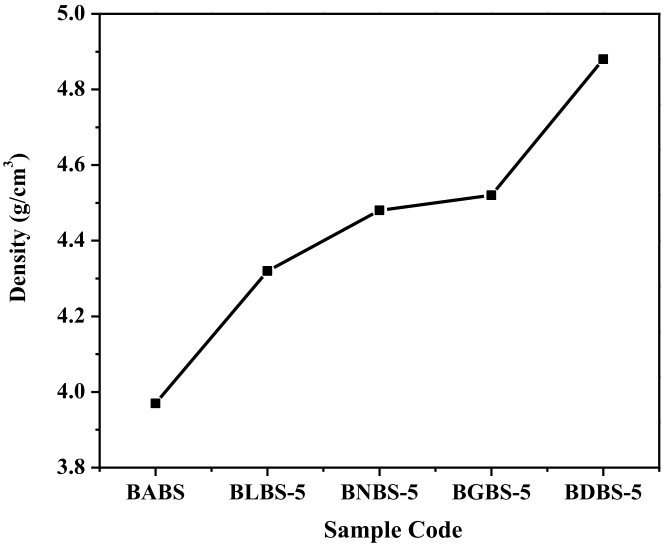

Fig. 2. Variation in the density (ρ) of 50BaO-(5-x) Al_2O_3-xR_2O_3–30B_2O_3–15SiO_2 (x = 0, 5 and R = Nd, Gd, La, Dy) glass-ceramics.

Arora et al. reported that in barium-based aluminosilicate glass–ceramics, barium aluminum silicate, $BaAl_2Si_2O_8$ (Hexagonal), is one of the major crystalline phases. It is observed that during heat treatment celsian ($BaAl_2Si_2O_8$) and hexacelsian (α-$BaAl_2Si_2O_8$) phases are formed. The increase in the duration of heat treatment transforms the hexacelsian phase into monoclinic celsian phase [12]. In some barium-based glass network, the hexacelsian and celsian phases are detected as minor phases [15]. With the addition of rare-earth oxides to the alumina borosilicate network, $RE_2Si_2O_7$ crystalline phases and other rare-earth based silicate phases are formed which results in high co-efficient of thermal expansion [16]. $LaBO_3$ crystalline phase is formed due to the tendency of $La^{3+}$to co-ordinate with triangular co-ordinated boron. Mahapatra et al. observed the crystalline phase ($LaBO_3$) in the devirtification of (25-x)SrO-20 La_2O_3-(7-x) Al_2O_3–40B_2O_3–8SiO_2 glass systems [17].

3.2. Density

The density of 50BaO-(5-x)Al_2O_3-xR_2O_3–30B_2O_3–15SiO_2 (x = 0, 5 and R = Nd, Gd, Dy, La) glass-ceramics is 3.92 g/cm^3 (BABS), 4.48 g/cm^3 (Nd_2O_3), 4.52 g/cm^3 (Gd_2O_3), 4.88 g/cm^3 (Dy_2O_3) and 4.32 g/cm^3 (La_2O_3). Density of glass-ceramics increases with the addition of rare earth oxides (Nd_2O_3, Gd_2O_3, Dy_2O_3 and La_2O_3) (Fig. 2). Glass-ceramic density is higher for Dy_2O_3 added glass-ceramics (4.88 g/cm^3) compared to that of Gd_2O_3 (4.52 g/cm^3), Nd_2O_3 (4.48 g/cm^3) and La_2O_3 (4.32 g/cm^3) based glass-ceramics. The increase in density of glass–ceramics is due to the formation of high density crystalline phases in it. The density is higher for the crystalline phases Dy_2SiO_5 (6.65 g/cm^3) and $Dy_2Si_2O_7$ (7.12 g/cm^3) than that of Gd_2SiO_5 (6.61 g/cm^3), $Gd_2Si_2O_7$ (5.93 g/cm^3), $Nd_2Si_2O_7$ (5.25 g/cm^3), La_3BO_6 (5.39 g/cm^3) and $LaBO_3$

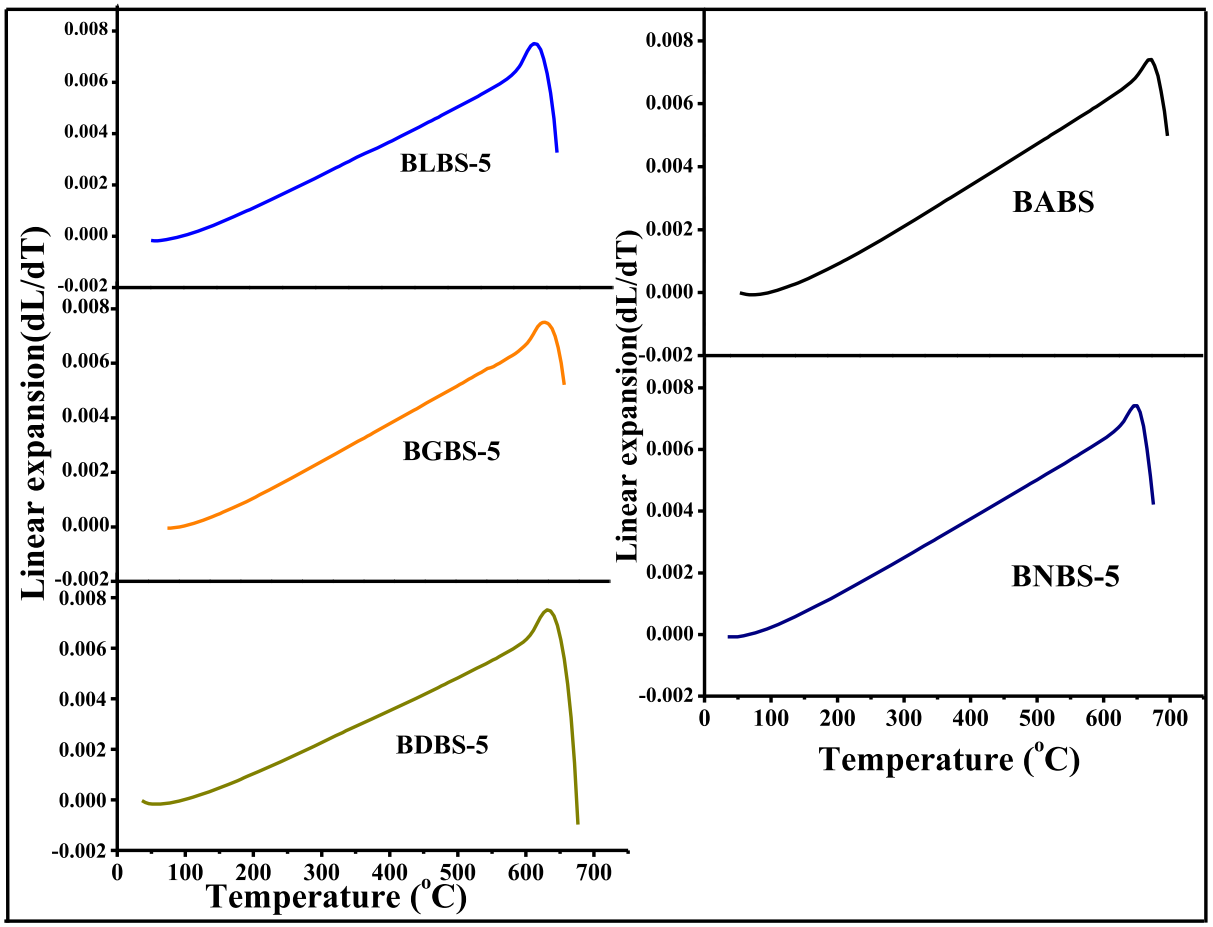

Fig. 3. Linear thermal expansion of 50BaO-(5-x) Al_2O_3-xR_2O_3–30B_2O_3–15SiO_2 (x = 0, 5 and R = Nd, Gd, La, Dy) glass-ceramics.

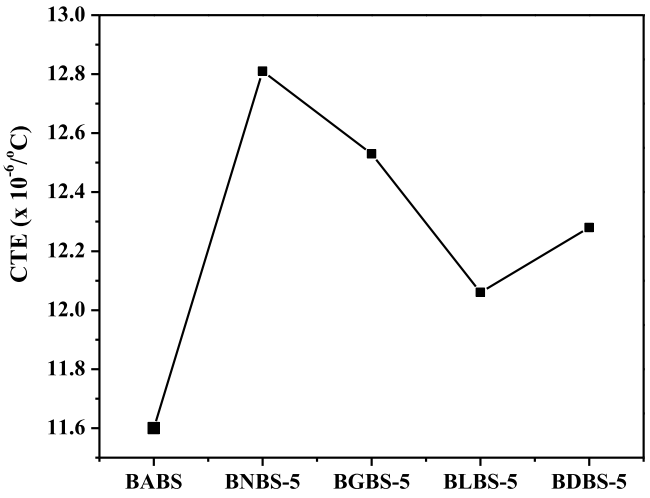

Fig. 4. Variation in thermal expansion of 50BaO-(5-x) Al_2O_3-xR_2O_3–30B_2O_3–15SiO_2 (x = 0, 5 and R = Nd, Gd, La, Dy) glass-ceramics.

(5.11 g/cm^3). Higher density results in the compactness of the network structure [18]. The increase in density depends not only with the crystalline phases but also with the increase in cationic field strength (CFS) of RE^{3+} ions. The density is higher for Dy_2O_3 based glass-ceramic due to the high CFS of Dy^{3+} (3.64 Å^{-2}) ion than that of Gd^{3+} (3.62 Å^{-2}), Nd^{3+} (3.41 Å^{-2}) and La^{3+} (2.81 Å^{-2}) ions. Increase in cationic field strength (CFS) implies densification of network structure, resulting in higher density [18,19].

3.3. Co-efficient of thermal expansion (CTE)

The linear thermal expansion curves of the glass-ceramics doped with rare earth oxides Nd_2O_3, Gd_2O_3, La_2O_3 and Dy_2O_3 are shown in Fig. 3. The co-efficient of thermal expansion (CTE) is calculated from the linear expansion curve by taking its slope. The variations of the co-efficient of thermal expansion for glass-ceramics are shown in Fig. 4. There is an increase in CTE of glass-ceramics with the addition of rare earth ions (Nd^{3+}, Gd^{3+}, La^{3+} and Dy^{3+}) in the network structure. The co-efficient of thermal expansion lies in the range (CTE) (11.60 – 12.81) x 10^{-6}/°C with the addition of rare earth ions (Nd^{3+}, Gd^{3+}, La^{3+} and Dy^{3+}) in the network structure. The co-efficient of thermal expansion (CTE) values are 11.60 × 10^{-6}/ °C for parent glass-ceramic (BABS) and 12.81 × 10^{-6}/ °C, 12.53 × 10^{-6}/ °C, 12.06 × 10^{-6}/ °C, 12.28 × 10^{-6}/ °C for Nd_2O_3, Gd_2O_3, La_2O_3 and Dy_2O_3 added glass-ceramics respectively. The CTE is higher for Nd_2O_3 added glass-ceramic as compared to that of La_2O_3, Dy_2O_3 and Gd_2O_3 added glass-ceramics.

The co-efficient of thermal expansion of glass-ceramics mainly depends on the nature and amount of crystalline phases and also micro structural arrangement of crystalline phases in the glass-ceramic matrix [20,21]. The lower CTE value of La_2O_3 added glass-ceramics compared to that of its base glass-ceramic is due to the low CTE of the crystalline phases formed. The borate based crystalline phases, La_3BO_6 and $LaBO_3$, have very low co-efficient of thermal expansion compared to that of silicate based crystalline phases. In the present glass-ceramics prepared silicate based crystalline phases are formed except La_2O_3 added system. The CTE increases for Nd_2O_3, $Gd_2O_3$and Dy_2O_3added glass-ceramics due to the presence of silicate based crystalline phases ($Dy_2Si_2O_7$ and Dy_2SiO_5, Gd_2SiO_5, $Gd_2Si_2O_7$, $Nd_2Si_2O_7$ and $Nd_4Si_3O_{12}$ for Dy_2O_3, Gd_2O_3 and Nd_2O_3added glass-ceramics respectively) having high CTE than the

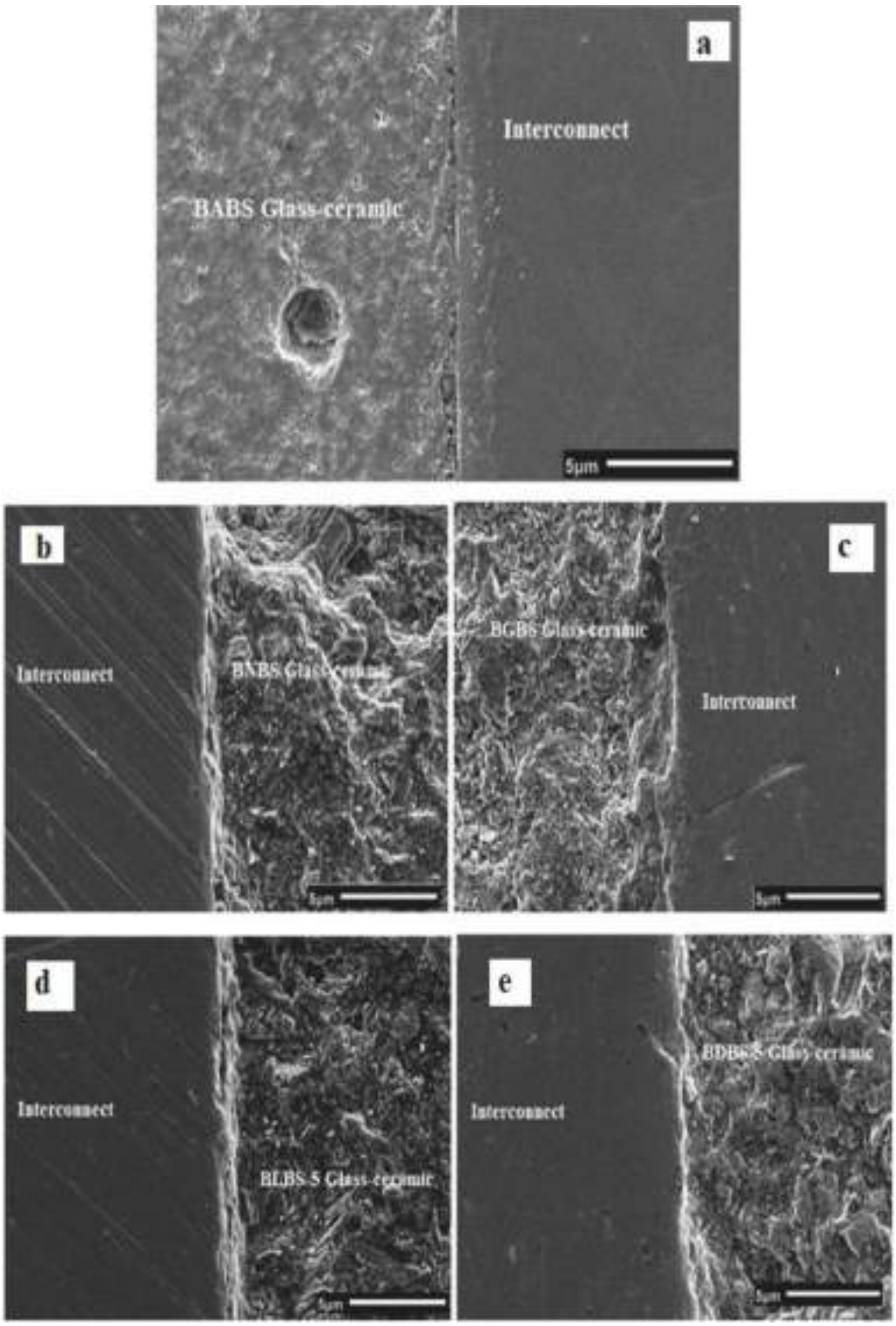

Fig. 5. . SEM images of the interface between glass-ceramics and Crofer22APU heat treated at 700 °C (a) BABS (b) BNBS-5 (c) BGBS-5 (d) BLBS-5 (e) BDBS-5.

borate phases. The co-efficient of thermal expansion of glass-ceramic mainly depends on the crystalline phase and volume of the crystalline phase in the glass-ceramic matrix [22–24]. The CTE values of the present glasses and glass-ceramics match with the requirement of a sealing material in SOFC applications (CTE = 9 – 13 × 10^{-6}/°C) [25].

3.4. Interaction studies

Bonding behavior of glass-ceramics with Crofer22APU has been investigated. Fig. 5 (a-e) represents a cross-sectional SEM image of the interface between the 50BaO-(5-x)Al_2O_3-xR_2O_3–30 B_2O_3–15SiO_2 ($x = 0$, 5 and R = Nd, Gd, Dy, La) glass-ceramics and Crofer22APU interconnect material after heat treatment at 700 °C for 10 h in oxidizing atmosphere. Two different zones are observed within the figure, one representing the

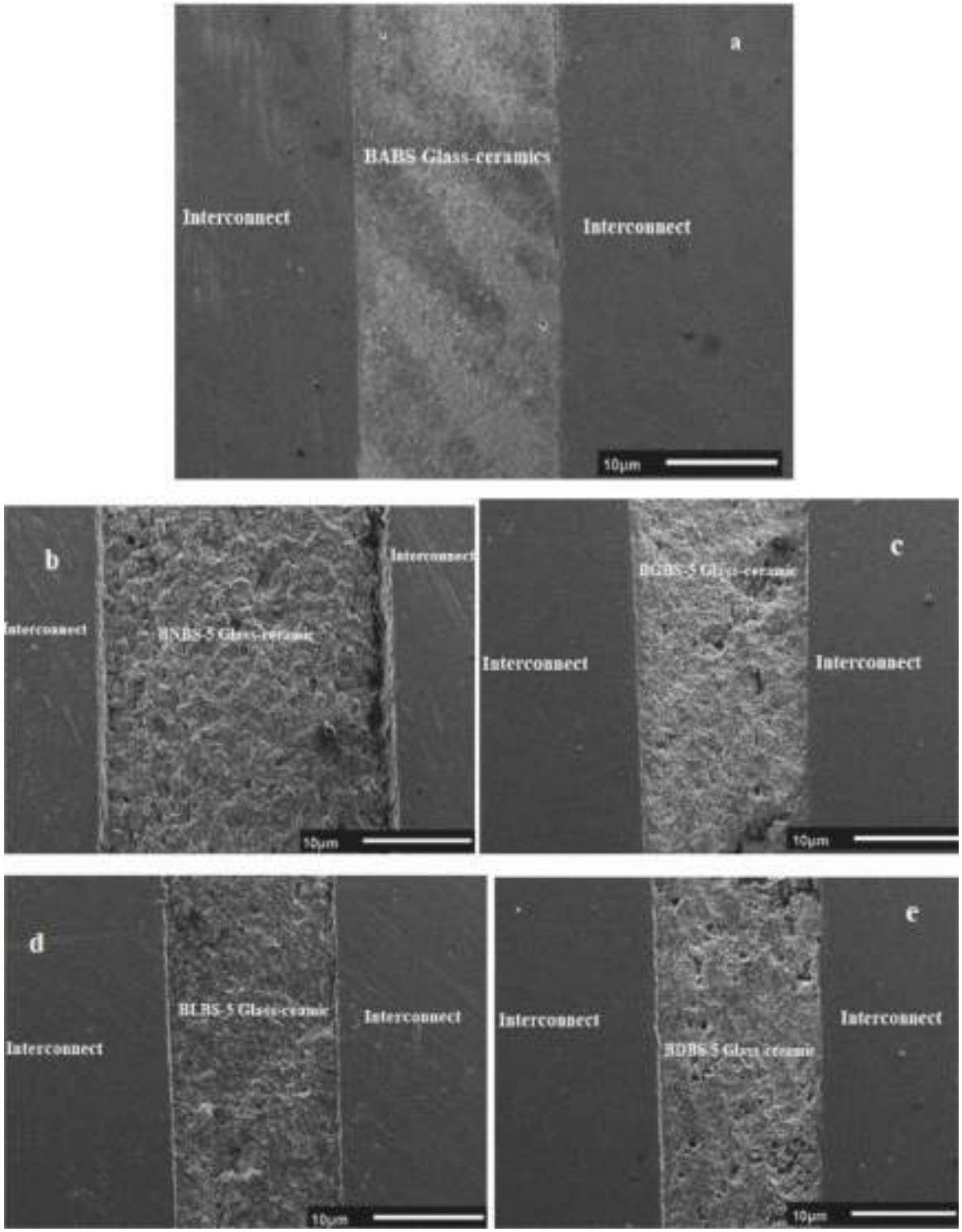

Fig. 6. . SEM images of Crofer22APU /glass-ceramics/Crofer22APU interface heat treated at 700 °C (a) BABS- (b) BNBS-5 (c) BGBS-5 (d) BLBS-5 (e) BDBS-5.

glass-ceramic sealant and therefore the other region represents the Crofer22APU. The high degree of bonding and compatibility at the interface means no obvious cracks are found on the interfaces. An honest adhesion between the glass-ceramic sealant and Crofer22APU interconnect is observed. An interface having continuous crack free surface indicates an honest physical compatibility between the two materials [26,27]. It is clear from Fig. 5(a-e) that, all the sealing glass-ceramics bonded well to the metallic part as no bubbles and cracks are observed at the interface. A limited inter diffusion of Cr and Ba across the boundary is observed, which is required permanently adhesion between metal and glass-ceramic [28]. Batfalsky et al. (2006) had reported that BaO containing glass-ceramics interacted chemically with chromia alloys forming $BaCrO_4$, which led to the separation of glass-ceramics from the alloy matrix which is due to the thermal expansion mismatch [29]. Within the present study, we don't observe a serious enhancement in Cr diffusion after heat treatment at 700 °C for 10 h and no adverse reactions at interface are observed. This is often a sign of the absence of $BaCrO_4$ phase formation. The micro structural study of the interfaces

Crofer22APU/glass-ceramic/Crofer22APU [Fig. 6(a-e)] showed that the interfaces remained joined together with no evidence of cracking suggesting good thermal compatibility between the glass-ceramic sealant and Crofer22APU [30]. The Crofer22APU/glass-ceramic/Crofer22APU interfaces are more or less defect free for this glass-ceramic composition when viewed after 10 h of warmth treatment at 700 °C glasses. All the sealing glass-ceramics bonded well to the metallic interconnect and no gaps are observed even at the sides of the joints. However, the Crofer22APU/glass-ceramic/Crofer22APU interfaces showed an interaction zone between the glass-ceramic and Crofer22APU interface at 700 °C temperature [30,31]. All the prepared glass-ceramics 50BaO-(5-x) Al_2O_3-xR_2O_3–30B_2O_3–15SiO_2 (R = Gd, Nd, Dy, La and x = 0, 5) contain B_2O_3 which may be a volatile material. Hence there's a chance of interaction of B_2O_3 at the glass-ceramic/Interconnect interface. Batfalsky et al. reported that the degradation of B_2O_3 containing sealants under humidified reducing conditions is due to the formation of volatile species [29]. But no such effects are observed within the present study. Further, since no chromate formation has been observed in any of the investigated diffusion couples, negligible chromium depletion are often expected at the phase boundary (Crofer22APU/Glass-ceramic).

4. Conclusions

Barium alumino borosilicate glasses with composition 50BaO-(5-x) Al_2O_3-xR_2O_3–30B_2O_3–15SiO_2 (x = 0, 5 and R = Nd, Gd, Dy, La) has been prepared by normal melt quench method successfully and converted to glass-ceramics by controlled crystallization. The density of glass-ceramics increases with the addition of Nd_2O_3, Gd_2O_3, Dy_2O_3 and La_2O_3. Glass-ceramic density is higher for Dy_2O_3 added glass-ceramics (4.88 g/cm^3) compared to that of Gd_2O_3 (4.52 g/cm^3), Nd_2O_3 (34.48 g/cm^3) and La_2O_3 (4.32 g/cm^3) based glass-ceramics. The increase in density of glass–ceramics is due to the formation of high density crystalline phases in it. The density is higher for the crystalline phases Dy_2SiO_5 (6.65 g/cm^3) and $Dy_2Si_2O_7$ (7.12 g/cm^3) than that of Gd_2SiO_5 (6.61 g/cm^3), $Gd_2Si_2O_7$ (5.93 g/cm^3), $Nd_2Si_2O_7$ (5.25 g/cm^3), La_3BO_6 (5.39 g/cm^3) and $LaBO_3$ (5.11 g/cm^3). There is an increase in CTE of glass-ceramics with the addition of rare earth ions (Nd^{3+}, Gd^{3+}, La^{3+} and Dy^{3+}) in the network structure. The co-efficient of thermal expansion lies in the range (CTE) (11.60 – 12.81) x 10^{-6}/°C for with the addition of rare earth ions (Nd^{3+}, Gd^{3+}, La^{3+} and Dy^{3+}) in the network structure. Glass-ceramics [50BaO-(5-x) Al_2O_3- xR_2O_3–30B_2O_3–15SiO_2 (R = Gd, Nd, Dy, La and x = 0, 5)] with Crofer22APU interface and Crofer22APU/Glass-ceramic/Crofer22APU sandwich model have been successfully synthesized. Glass-ceramic/Crofer22APU interface and Crofer22APU/Glass-ceramic/Crofer22APU sandwich model subjected to 700 °C for 10 h in air atmosphere showed no evidence of interfacial failure and cracks. All the presently prepared glass-ceramic seals have shown good adhesion with Crofer22APU interconnect. The seals are found intact after heat treatment at 700 °C for 10 h. The 50BaO-(5-x) Al_2O_3- xR_2O_3–30B_2O_3–15SiO_2 (R = Gd, Nd, Dy, La and x = 0, 5) glass-ceramics have no major enhancement in Cr diffusion and no adverse reactions at interface. Hence the presently prepared glass-ceramics can be used as sealant material in SOFC applications due to the matching of co-efficient of thermal expansion with the other components of SOFC and no adverse reactions at interface.

Author confirmation

All authors listed have made a significant contribution to the research reported and have read and approved the submitted manuscript, and furthermore, all those who made substantive contributions to this work have been included in the author list.

Declaration of Competing Interest

The authors declare that they have no known competing financial interests or personal relationships that could have appeared to influence the work reported in this paper.

Acknowledgments

The authors would like to acknowledge SRM University, Chennai for providing the facility for XRD in our study.

References

[1] T. Zhang, Q. Zou, Tuning the thermal properties of borosilicate glass ceramic seal forsolid oxide fuel cells, J. Europ. Ceram. Soc. 32 (2012) 4009–4013.
[2] Y.S. Chou, E.C. Thomsen, J.P. Choi, J.W. Stevenson, Compliant alkali silicate sealing glass for solid oxide fuel cell applications: the effect of protective YSZ coating on electrical stability in dual environment, J. Power Sources 202 (2012) 149–156.
[3] Y.S. Chou, J.W. Stevenson, R.N. Gow, Novel alkaline earth silicate sealing glass for SOFC Part 1. The effect of nickel oxide on the thermal and mechanical properties, J. Power Sources 168 (2007) 426–433.
[4] G. Kaur, O.P. Pandey, K. Singh, Chemical interaction study between lanthanum based different alkaline earth glass sealants with Crofer22APU for solid oxide fuel cell applications, Int. J. Hydrog. Energy 37 (2012) 3883–3889.
[5] F. Smeacetto, A. De Miranda, A. Chrysanthou, E. Bernardo, M. Secco, M. Bindi, M. Salvo, A.G. Sabato, M. Ferraris, Novel glass-ceramic composition as sealant for SOFCs, J. Am. Ceram. Soc. 97 (12) (2014) 3835–3842.
[6] Z. Dai, J. Pu, D. Yan, B. Chi, L. Jian, Thermal cycle stability of Al_2O_3-based compressive seals for planar intermediate temperature solid oxide fuel cells, Int. J. Hydrog. Energy 36 (2011) 3131–3137.
[7] B. Dev, M.E. Walter, G.B. Arkenberg, S.L. Swartz, Mechanical and thermal characterization of a ceramic/glass composite seal for solid oxide fuel cells, J. Power Sources 245 (2014) 958–966.
[8] B. Tiwari, A. Dixit, G.P. Kothiyal, Study of glasses/glass-ceramics in the SrO-ZnO-SiO_2 system as high temperature sealant for SOFC applications, Int. J. Hydrog. Energy 36 (2011) 15002–15008.
[9] S.B. Sohn, S.Y. Choi, G.H. Kim, H.S. Song, G.D. Kim, J. Non-Cryst. Solids 297 (2–3) (2002) 103–112.
[10] K.L. Ley, M. Krumpelt, R. Kumar, M. Jh, I. Bloom, Glass-ceramic sealants for solid oxide fuel cells: part I. Physical properties, J. Mater. Res. 11 (6) (1996) 1489–1493.
[11] Yang Z., Coyle C.A., Baskaran S., Chick L.A., Gas-tight metal/ceramic or metal/metal seals for application in high temperature electrochemical devices and method of making, *U.S. Patent No. 6,843,406*, B2, 2005, Washington, DC: U.S. Patent and Trademark Office.
[12] A. Arora, K. Singh, O.P. Pandey, Thermal, structural and crystallization kinetics of SiO_2-BaO-ZnO-B_2O_3-Al_2O_3 glass samples as a sealant for SOFC, Int. J. Hydrog. Energy 36 (2011) 14948–14955.
[13] D. Bahadur, N. Lahl, K. Singh, L. Singheiser, K. Hilpertz, Influence of nucleating agents on the chemical interaction of MgO- Al_2O_3- SiO_2- B_2O_3 glass sealants with components of SOFCs, J. Electrochem. Soc. 151 (4) (2004) A558–A562.
[14] F. Lofaj, R. Satet, M.J. Hoffmann, A.R.A. Lopez, Thermal expansion and glass transition temperature of the rare earth doped oxynitride glasses, J. Euro. Ceram. Soc. 24 (2004) 3377–3385.
[15] V. Kumar, A. Arora, O.P. Pandey, K. Singh, Studies on thermal and structural properties of glasses as sealants for solid oxide fuel cells, Int. J. Hydrog. Energy 33 (1) (2008) 434–438.
[16] J. Puig, F. Ansart, P. Lenormand, L. Antoine, J. Dailly, Sol-gel synthesis and characterization of barium (magnesium) aluminosilicate glass sealants for solid oxide fuel cells, J. Non-Cryst. Solids 357 (2011) 3490–3494.
[17] M.K. Mahapatra, K. Lu, W.T. Reynolds Jr, Thermophysical properties and devitrification of SrO - La_2O_3 - Al_2O_3 - B_2O_3 - SiO_2 -based glass sealant for solid oxide fuel/electrolyzer cells, J. Power Sources 179 (1) (2008) 106–112.
[18] Y.R. Luo, Hand Book of Bond Dissociation Energies in Organic Compounds, 66, CRC Press, New York, Washington DC, 2002.
[19] Salinigopal M.S., Gopakumar N., Anjana P.S., *Silicon* Alkaline earth based borosilicate glasses as sealants in solid oxide fuel cell applications, 12, 2020, 101–107.
[20] Z. Xiao, J. Zhou, Y. Wang, M. Luo, Microstructure and properties of LiO_2-Al_2O_3-SiO_2-P_2O_5 glass-ceramics, Open Mater. Sci. J. 5 (2011) 45–50.
[21] M. Garai, N. Sasmal, B. Karmakar, Effects of M^{2+} (M = Ca, Sr and Ba) Addition on Crystallization and Microstructure of SiO_2-MgO-Al_2O_3-B_2O_3-K_2O-F Glass, Ind. J. Mater. Sci. 638341 (1) (2015) 1–8.
[22] H. Darwish, M.M. Gomaa, Effect of compositional changes on the structure and properties of alkali-alumino borosilicate glasses, J. Mater. Sci 17 (1) (2006) 35–42.
[23] M.S. Salinigopal, N. Gopakumar, P.S. Anjana, Synthesis and characterization of 50 BaO –(5-x) Al_2O_3 –xR_2O_3 –30 B_2O_3 –15 SiO_2(x = 0, 1, 2, 3, 4, 5 and R = Nd, Gd) glass-ceramics, J. Non-Cryst. Solids 535 (2020), 119956.
[24] N.S. Weiss, R.E. Youngman, R. Thorpe, N.J. Smith, E.M. Pierce, A. Goel, An insight into the corrosion of alkali aluminoborosilicate glasses in acidic environments, Phys. Chem. Chem. Phys. 22 (2020) 1881–1896.
[25] A.A. Reddy, D.U. Tulyaganov, M.J. Pascual, V.V. Kharton, E.V. Tsipis, V. A. Kolotygin, J.M.F. Ferreira, Diopside-Ba disilicate glass-ceramic sealants for SOFC: enchanced adhesion and thermal stability by Sr for Ca substitution, Int. J. Hydrog. Energy 38 (2013) 3073–3086.

[26] C.K. Lin, J.Y. Chen, J.W. Tian, L.K. Chiang, S.H. Wu, Joint strength of a solid oxide fuel cell glass-ceramic sealant with metallic interconnect, J. Power Sources 205 (2012) 307–317.
[27] Y. Ye, D. Yan, X. Wang, J. Pu, B. Chi, L. Jian, Development of novel glass-based composite seals for planar intermediate temperature solid oxide fuel cells, Int. J. Hydrog. Energy. 37 (2012) 1710–1716.
[28] K. Sharma, G.P. Kothiyal, L. Montagne, F.O. Mear, B. Revel, A new formulation of barium-strontium silicate glasses and glass-ceramics for high-temperature sealant, Int. J. Hydrog. Energy 37 (2012) 11360–11369.
[29] P. Batfalsky, V.A.C. Haanappel, J. Malzbender, N.H. Menzler, V. Shemet, I. C. Vinke, R.W. Strinbrench, Chemical interaction between glass-ceramic sealants and interconnect steels in SOFC stacks, J. Power Sources 155 (2) (2006) 128–137.
[30] F. Smeacetto, A. Chrysanthou, M. Salvo, T. Moskalewicz, F.D. Bytner, L.C. Ajitdoss, M. Ferraris, Thermal cycling and ageing of a glass-ceramic sealant for planar SOFCs, Int. J. Hydrog. Energy 36 (2011) 11895–11903.
[31] S. Ghosh, A.D. Sharma, A.K. Mukhopadhyay, P. Kundu, R.N. Basu, Int. J. Hydrog. Energy 35 (2010) 272–283.